J Adv Manuf Eng, Vol. 5, Issue. 1, pp. 9–14, March, 2024

Journal of Advances in Manufacturing Engineering
Web page info: https://jame.yildiz.edu.tr
DOI: 10.14744/ytu.jame.2024.00002

Original Article

Corrosion inhibition of AlSi10Mg additively manufactured parts in 3.5% NaCl solution

Burçin ÖZBAY KISASÖZ*

Fatih Sultan Mehmet Vakıf University, Aluminium Test Training and Research Center (ALUTEAM), İstanbul, Türkiye

ARTICLE INFO

Article history
Received: 10 January 2024
Accepted: 25 March 2024

Key words:
AlSi10Mg, corrosion, laser powder bed fusion (LPBF), inhibition.

ABSTRACT

In this study, corrosion inhibition of the additively manufactured AlSi10Mg was investigated in 3.5% NaCl solution with the addition of 1% and 3% NH_4NO_3. The potentiodynamic polarization and electrochemical impedance spectroscopy tests were performed in order to reveal the corrosion behavior of the AlSi10Mg. The corrosion inhibition behavior of the AlSi10Mg was determined by analyzing the Tafel curves, phase angle/frequency curves and equivalent circuit results. Moreover, microstructures of the produced sample and corroded surfaces were investigated with light metal microscopy. It was stated that the corrosion rate value of the AlSi10Mg is reduced with the presence of NO_3^- in 3.5% NaCl solution. On the other hand, the surface/solution interaction was reduced by adding NH_4NO_3 into 3.5% NaCl solution. It can be clearly emphasized that using 3% NH_4NO_3 is quite effective in improving the corrosion behavior of AlSi10Mg in 3.5% NaCl.

Cite this article as: Özbay Kısasöz, B. (2024). Corrosion inhibition of AlSi10Mg additively manufactured parts in 3.5% NaCl solution. *J Adv Manuf Eng*, 5(1), 9–14.

INTRODUCTION

Additive manufacturing (AM) is a promising manufacturing process to produce metallic parts with desired properties. Laser powder bed fusion (LPBF) is one of the AM methods, and metallic powders are deposited layer-by-layer with a laser beam [1–3].

AlSi10Mg alloy has often been used in the conventional casting process. The chemical composition of the alloy is near eutectic, and AlSi10Mg has lower shrinkage and higher fluidity owing to its chemical composition. Besides, AlSi10Mg is also of interest for additive manufacturing processes, and AlSi10Mg has been widely used in LPBF process [4–7].

The LPBF AlSi10Mg parts exhibit higher mechanical properties compared to conventional cast parts. Manfredi et al. [8] stated that LPBF AlSi10Mg parts have higher yield strength and hardness values compared to conventional A360 alloy. It was revealed that the LPBF process provides the fine distribution of silicon and grain refinement due to the rapid cooling of the structure [9, 10]. Moreover, besides mechanical properties, the LPBF AlSi10Mg's corrosion properties are also crucial. It has been observed that the corrosion resistance of aluminium alloys produced by AM processes is equal to or slightly higher than conventional casting techniques [11–13]. Chen et al. [14] determined that the LPBF process improves the corrosion resistance of Al-12Si alloy in 3.5% NaCl, compared to the as-cast condition.

On the other hand, various have been carried out to improve the corrosion resistance of the LPBF AlSi10Mg. Surface treatments, like chemical etching, sand blasting and shot peening are applied to LPBF alloy to obtain higher corrosion resistance [15–18]. It was also reported that the usage of corrosion inhibitors can slow down the corrosion reactions and reduce corrosion damage in the AlSi10Mg parts [19–22].

***Corresponding author.**
*E-mail address: burcinozbay@gmail.com

Table 1. The chemical composition of the AlSi10Mg powder (wt.%)

Si	Fe	Mg	Cu	Ni	Mn	Zn	Pb	Ti	Al
9.8	0.14	0.36	0.02	0.01	0.01 (max)	0.01 (max)	0.01 (max)	0.01	Bal.

Si: Silicium; Fe: Iron; Mg: Magnesium; Cu: Copper; Ni: Nickel; Zn: Zinc; Pb: Lead; Ti: Titanium; Al: Aliminium.

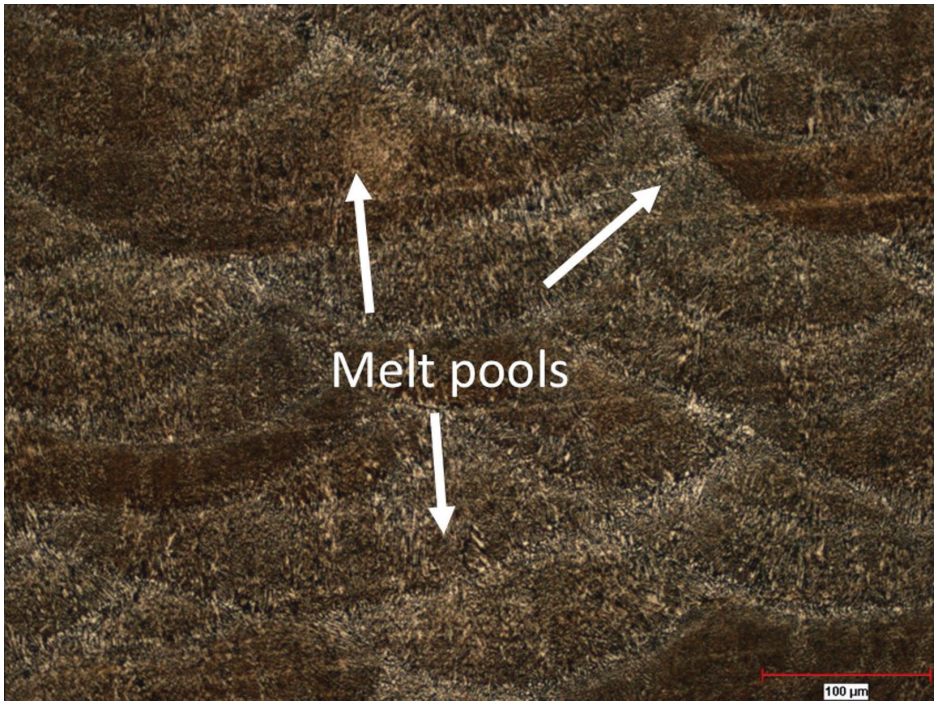

Figure 1. The microstructure of the AlSi10Mg is parallel to the building direction in LPBF.

This study revealed the influence of corrosion inhibition of ammonium nitrate on LPBF AlSi10Mg. The electrochemical tests were performed in 3.5% NaCl solution with various ammonium nitrate content. Electrochemical impedance spectroscopy (EIS) and Tafel analyses were carried out in each test solution. Moreover, the corroded surface of the samples was investigated.

MATERIALS AND METHODS

AlSi10Mg powders were used in LPBF process. Samples were produced with EOS M290 system. The average particle size of the AlSi10Mg powders was determined as 47±0.4 µm by Malvern 3000 mastersizer. The chemical composition of the powder was given in Table 1.

Microstructure characterization of the produced samples was carried out by light metal microscopy (LMM) (Zeiss Axio Lab.A), and the corroded surface of the samples was also observed with LMM analysis. Corrosion inhibition of the AlSi10Mg AM alloy was studied in 3.5% NaCl, 3.5% NaCl + 1% NH_4NO_3, and 3.5% NaCl + 3% NH_4NO_3 solutions, respectively. The test solutions were in open to air condition. The corrosion behavior of the alloy was investigated by potentiodynamic polarization (PDP) and electrochemical impedance spectroscopy (EIS) tests. The corrosion tests were repeated at least three times until all repeated runs exhibited similar polarization curves. The tests were performed with Ivium Compactstat with a triple electrode system consisting of a reference electrode (Ag/AgCl solution), a working electrode (test sample), and a counter electrode (platinum). Prior to the PDP and EIS tests, an open circuit potential (OCP) of the samples was investigated by holding samples in the test solutions for 30 minutes. Corrosion potential (E_{corr}), corrosion current density (i_{corr}), and corrosion rate values were obtained using Tafel curves following the PDP tests. Moreover, the EIS tests were performed, the samples' phase angle/frequency curves were obtained, and the test results were examined with the fitted equivalent circuit.

RESULTS AND DISCUSSION

Figure 1 shows the microstructure of the AlSi10Mg produced by LPBF. The AM microstructure consisted of melt pools and fish-scale pattern. The melt pools were characteristic microstructure of the LPBF process, and layer-by-layer deposition also provided the formation of fish-scale patterns [23]. It can be deduced from the Figure 1 that the samples were successfully produced by the LPBF process.

The Tafel curves and PDP test results are in Figure 2 and Table 2, respectively. An active behavior was observed in solution of 3.5% NaCl and 3.5% NaCl + 1% NH_4NO_3, while

Table 2. Potentiodynamic polarization test results

Sample	E_{corr} (V)	i_{corr} (A·cm^{-2})	Corrosion rate (mm·year^{-1})
3.5% NaCl	-0.7309	1.95·10^{-6}	0.01753
3.5% NaCl + 1% NH_4NO_3	-0.7085	0.98·10^{-6}	0.01104
3.5% NaCl + 3% NH_4NO_3	-0.6285	0.19·10^{-6}	0.00217

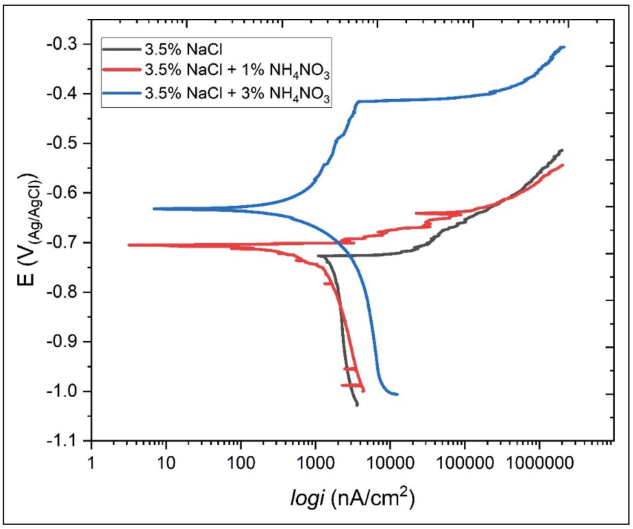

Figure 2. Potentiodynamic polarization curves.

the curve in 3.5% NaCl + 3% NH_4NO_3 solution showed a pseudo passive zone. The usage of NH_4NO_3 as an inhibitor significantly improved the corrosion behavior of the alloy. The E_{corr} and i_{corr} values of the AlSi10Mg in 3.5% NaCl solution were determined as -0.7309 V and 1.95·10^{-6} A·cm^{-2}, respectively. Using NH_4NO_3 with 1% and 3% in NaCl solution increased the E_{corr} to -0.7085 V and -0.6285 V, respectively. In particular, the usage of 3% NH_4NO_3 significantly increased the E_{corr} and delayed the occurrence of corrosion on the AlSi10Mg surface.

Moreover, the presence of NH_4NO_3 reduced i_{corr} and dissolution of the surface. The i_{corr} value of 1.95·10^{-6} A·cm^{-2} in 3.5% solution decreased to 0.19·10^{-6} A·cm^{-2} in 3.5% NaCl + 3% NH_4NO_3 solution. Accordingly, corrosion rate values were found as 0.01753 mm·year^{-1}, 0.01104 mm··year^{-1} and 0.00217 mm·year^{-1} in 3.5% NaCl, 3.5% NaCl + 1% NH_4NO_3, and 3.5% NaCl + 3% NH_4NO_3 solutions, respectively. The usage of NH_4NO_3 not only delayed the formation of corrosion on AlSi10Mg surface but also decreased the dissolution rate of the surface and reduced the corrosion rate.

The microstructures of the corroded surfaces after the PDP tests performed in all three solutions are shown in Figure 3. In the presence of Cl^- ions, corrosion damage on the surface of aluminium alloys occurs in the form of pitting. Although pitting damage was visible on all three surfaces, the pits formed intensely, and severe surface damages were observed on the surface of the AlSi10Mg in 3.5% NaCl solution (Fig. 3a). It was observed that the surface damage was reduced, and the formation of pit was decreased with the presence of NH_4NO_3 in the test solution.

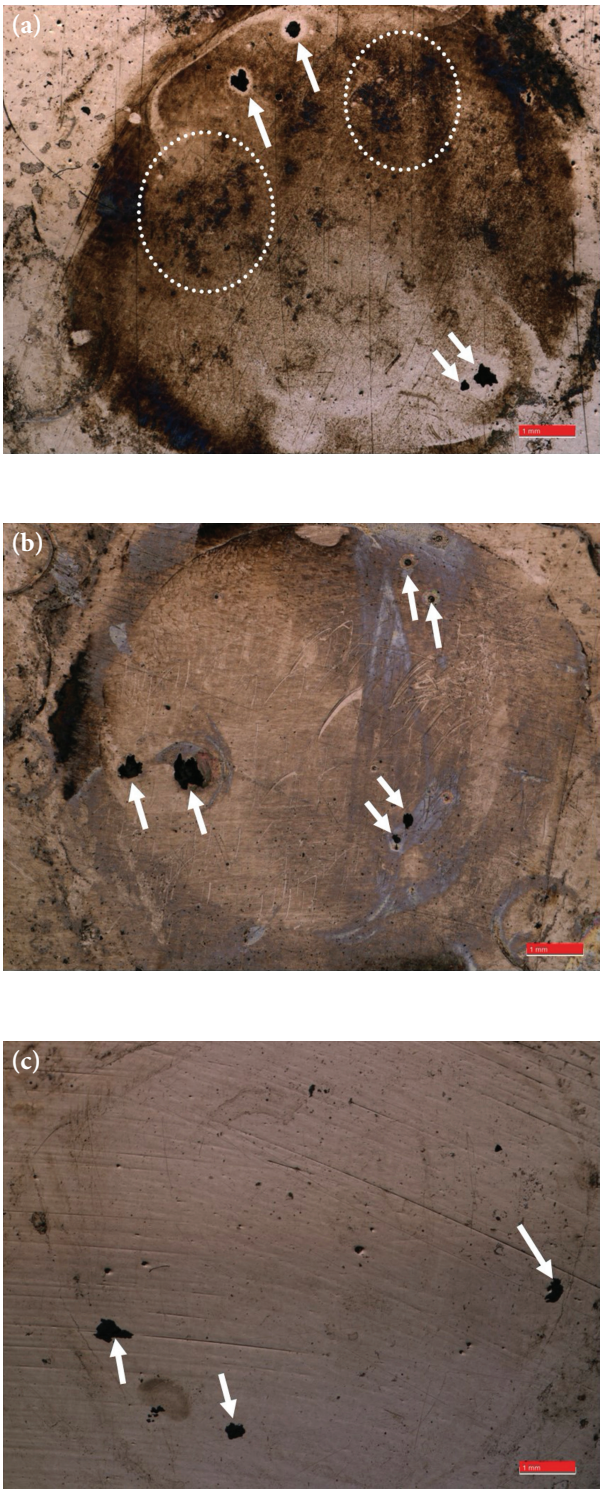

Figure 3. Surface microstructure of the samples after PDP tests **(a)** in 3.5% NaC, **(b)** in 3.5% NaCl + 1% NH_4NO_3, and **(c)** 3.5% NaCl + 3% NH_4NO_3.

Table 3. Fitted equiavalent circuit results

Sample	$R_{solution}$ (Ω·cm²)	$R_{substrate}$ (Ω·cm²)	n	$CPE_{substrate}$, Y_0 $(\Omega^{-1}\cdot cm^{-2}\cdot s^a)^n$
3.5% NaCl	24.15	5.596×10^3	0.946	6.881×10^{-6}
3.5% NaCl + 1% NH_4NO_3	24.07	6.146×10^3	0.909	4.347×10^{-6}
3.5% NaCl + 3% NH_4NO_3	22.28	6.461×10^3	0.901	3.185×10^{-6}

In the corrosion of aluminium with Cl^- ions, the oxide layer initially reacts with the Cl^- ions and the oxide film is thinned. Also, aluminium chloride-based products are formed, and exposure of the bare aluminium surface occurs. In the presence of NO_3^- ions, NO_3^- provides a corrosion retarding effect by reducing the free aluminium surface. The corrosion reactions on the AlSi10Mg surface in the presence of NO_3^- ions can be expressed as follows [24]:

$$Al^{3+} + 2Cl^- + 2H_2O = Al(OH)_2Cl_2^- + 2H^+ \quad (1)$$
$$Al = Al^{3+} + 3e^- \quad (2)$$
$$Al^{3+} + 4Cl^- = AlCl_4^- \quad (3)$$
$$AlCl_4^- + 2H_2O = Al(OH)_2Cl + 2H^+ + 3Cl^- \quad (4)$$
$$3NO_3^- + 8Al + 18H_2O = 3NH_3 + 8Al(OH)_3 + 3OH^- \quad (5)$$

The aluminum passivation was provided with the presence of in NH_4NO_3 test solution. NO_3^- reduced the anodic current density, and the corrosion behavior of the AlSi10Mg was improved. Moreover, the pitting potential (E_{pit}) of the AlSi10Mg was increased with the NO_3^-, and the pitting potential values in 3.5% NaCl, 3.5% NaCl + 1% NH_4NO_3, and 3.5% NaCl + 3% NH_4NO_3 solutions were determined as -0.687 V, -0.663 V and -0.418 V, respectively. It can be deduced that the 3% NH_4NO_3 was quite effective to improve corrosion behavior of AlSi10Mg in 3.5% NaCl.

The EIS curve and fitted equivalent circuit are given in Figure 4, and the fitted equivalent circuit results are summarized in Table 3. The maximum peak angles for all test solutions were detected in the medium frequency range. These maximum peak angles in the medium frequency range can be attributed to the protective aluminium oxide layer. It can be stated that the phenomenon is more apparent for the short time of corrosion exposure. $R_{solution}$, $R_{substrate}$, and $CPE_{substrate}$ represented the solution resistance, substrate (AlSi10Mg) resistance, and capacitance of the substrate (AlSi10Mg), respectively. The measured capacitance was often not ideal, and Q was determined as the constant phase element. The $R_{solution}$ was obtained at similar values since the tests were carried out in the 3.5% NaCl solution. However, the addition of NH_4NO_3 reduced the solution resistance in a small manner. It was observed that the changes in $R_{substrate}$ values were also in small manner. But then it can be stated that the increasing trend of the $R_{substrate}$ with the increasing NH_4NO_3 content of the solution can be attributed to improved corrosion resistance of the AlSi10Mg surface.

Moreover, $Q_{substrate}$ value was reduced with increasing NH_4NO_3 content of the solution, and it indicated that the solution/substrate interaction is decreased with the presence of the NH_4NO_3. The obtained results obtained were consistent with the PDP test results. The presence of

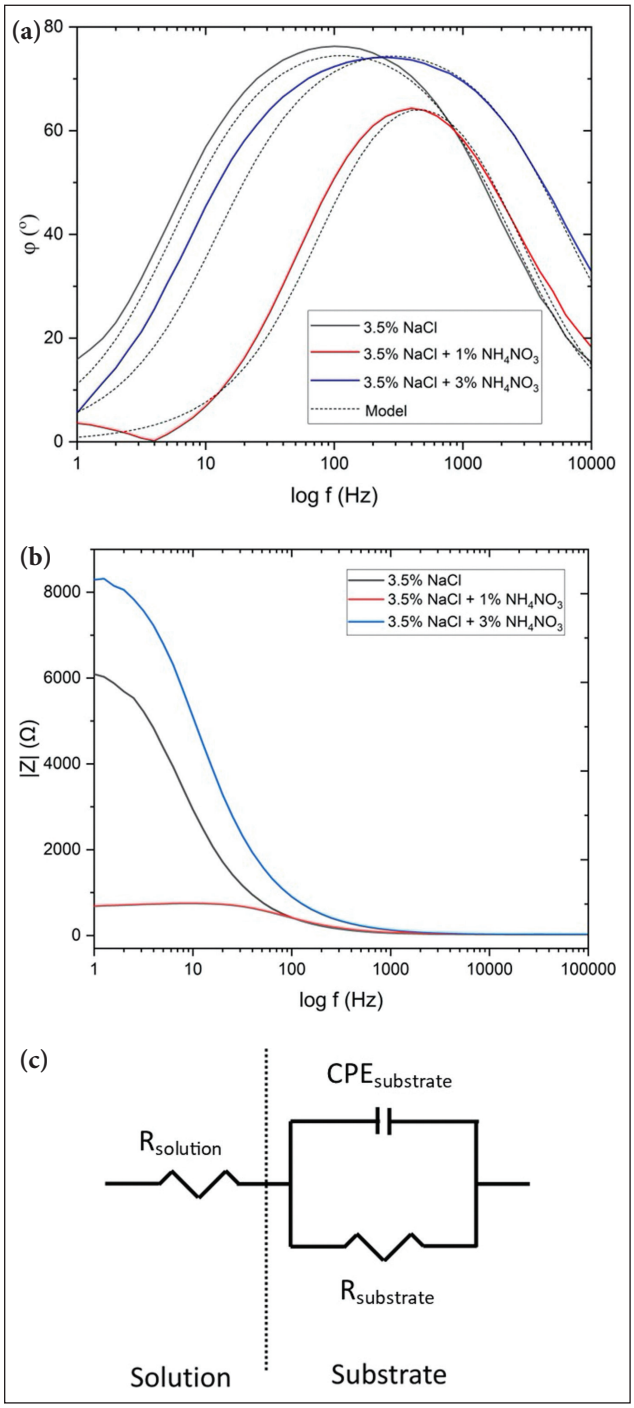

Figure 4. EIS test results **(a)** and **(b)** Bode plots, **(c)** Fitted equivalent circuit.

NO_3^- in the solution provides the reduction of aluminium during the corrosion process, which reduces the solution/material interaction.

CONCLUSION

The AlSi10Mg samples were produced successfully by the LPBF process. Also, the inhibition behavior of the AlSi10Mg AM samples was investigated in 3.5% NaCl solution with the addition of NH_4NO_3.

The addition of NH_4NO_3 improves the E_{corr} and i_{corr} values of the AlSi10Mg, and it was observed that the corrosion rate value of the AlSi10Mg is reduced with the presence of NO_3^- in 3.5% NaCl solution.

Moreover, the presence of NH_4NO_3 increased the resistance of the surface, reduced the surface/solution interaction and the corrosion resistance was improved with reduction of the aluminium by NO_3^-.

Data Availability Statement

The authors confirm that the data that supports the findings of this study are available within the article. Raw data that support the finding of this study are available from the corresponding author, upon reasonable request.

Conflict of Interest

The authors declared no potential conflicts of interest with respect to the research, authorship, and/or publication of this article.

Use of AI for Writing Assistance

Not declared.

Ethics

There are no ethical issues with the publication of this manuscript.

REFERENCES

[1] Cabrini, M., Lorenzi, S., Pastore, T., Testa, C., Manfredi, D., Cattano, G., & Calignano, F. (2018). Corrosion resistance in chloride solution of the AlSi10Mg alloy obtained by means of LPBF. *Surface and Interface Analysis, 51*(12), 1159–1164. [CrossRef]

[2] Frazier, W. E. (2014). Metal additive manufacturing: A review. *Journal of Materials Engineering and Performance, 23*(6), 1917–1928. [CrossRef]

[3] Louvis, E., Fox, P., & Sutcliffe, C. J. (2011). Selective laser melting of aluminium components. *Journal of Materials Processing Technology, 211*(2), 275–284. [CrossRef]

[4] Cabrini, M., Calignano, F., Fino, P., Lorenzi, S., Lorusso, M., Manfredi, D., Testa, C., & Pastore, T. (2018). Corrosion behavior of heat-treated AlSi10Mg manufactured by laser powder bed fusion. *Materials, 11*(7), Article 1051. [CrossRef]

[5] Leon, A., & Aghion, E. (2017). Effect of surface roughness on corrosion fatigue performance of AlSi10Mg alloy produced by Selective Laser Melting (SLM). *Materials Characterization, 131*, 188–194. [CrossRef]

[6] Wu, J., Wang, X. Q., Wang, W., Attallah, M. M., & Loretto, M. H. (2016). Microstructure and strength of selectively laser melted AlSi10Mg. *Acta Materialia, 117*, 311–320. [CrossRef]

[7] Neuser, M., Grydin, O., Frolov, Y., & Schaper, M. (2022). Influence of solidification rates and heat treatment on the mechanical performance and joinability of the cast aluminum alloy AlSi10Mg. *Production Process, 16*, 193–202. [CrossRef]

[8] Manfredi, D., Calignano, F., Manickavasagam, K., Canali, R., Ambrosio, E. aP., & Atzeni, E. (2013). From powders to dense metal parts: Characterization of a commercial AlSiMg alloy processed through direct metal laser sintering. *Materials, 6*, 856–869. [CrossRef]

[9] Olakanmi, E. O. (2013). Selective laser sintering/melting (SLS/SLM) of pure Al, Al–Mg, and Al–Si powders: Effect of processing conditions and powder properties. *Journal of Materials Processing Technology, 213*, 1387–1415. [CrossRef]

[10] Read, N., Wang, W., Essa, K., & Attallah, M. M. (2015). Selective laser melting of AlSi10Mg alloy: Process optimisation and mechanical properties development. *Materials & Design, 65*, 417–424. [CrossRef]

[11] Leon, A., Shirizly, A., & Aghion, E. (2016). Corrosion behavior of AlSi10Mg alloy produced by additive manufacturing (AM) vs. its counterpart gravity cast alloy. *Metals, 6*(7), Article 148. [CrossRef]

[12] Fathi, P., Mohammadi, M., Duan, X., & Nasiri, A. M. (2018). A comparative study on corrosion and microstructure of direct metal laser sintered AlSi10Mg_200C and die-cast A360.1 aluminum. *Journal of Materials Processing Technology, 259*, 1–14. [CrossRef]

[13] Gharbi, O., Jiang, D., Feenstra, D. R., Kairy, S. K., Wu, Y., Hutchinson, C. R., & Birbilis, N. (2018). On the corrosion of additively manufactured aluminium alloy AA2024 prepared by selective laser melting. *Corrosion Science, 143*, 93–106. [CrossRef]

[14] Chen, Y., Zhang, J., Gu, X., Dai, N., Qin, P., & Zhang, L. (2018). Distinction of corrosion resistance of selective laser melted Al-12Si alloy on different planes. *Journal of Alloys and Compounds, 747*, 648–658. [CrossRef]

[15] Maleki, E., Unal, O., Bandini, M., Guagliano, M., & Bagherifard, S. (2022). Individual and synergistic effects of thermal and mechanical surface post-treatments on wear and corrosion behavior of laser powder bed fusion AlSi10Mg. *Journal of Materials Processing Technology, 302*, Article 117479. [CrossRef]

[16] Maleki, E., Bagherifard, S., Rovatti, L., Ishola, R.M., Revuru, M., & Guagliano, M. (2023). Developing a best practice for sample preparation of additive manufactured AlSi10Mg for electron backscatter diffraction analysis. *Additive Manufacturing Letters, 5*, Article 100122. [CrossRef]

[17] Avanzini, A., Battini, D., Gelfi, M., Girelli, L., Petrogalli, C., Pola, A., & Tocci, M. (2019). Investigation on fatigue strength of sand-blasted DMLS-AlSi10Mg alloy. *Procedia Structural Integrity, 18*, 119–128. [CrossRef]

[18] Rauito, T., Hamada, A., Kumpula, J., & Jarvenpaa, A. (2022). The effect of shot peening on corrosion performance of anodized laser powder bed fusion manufactured AlSi10Mg. *IOP Conference Series: Materials Science and Engineering, 1234*, Article 012035. [CrossRef]

[19] Valentini, F., Pezzato, L., Dabalà, M., & Brunelli, K. (2023). Study of the effect of functionalization with inhibitors on the corrosion properties of PEO-coated additive manufactured AlSi10Mg alloy. *Journal of Materials Research and Technology, 27*(11–12), 3595–3609. [CrossRef]

[20] Duchardt, T., Andersohn, G., & Oechsner, M. (2015). Corrosion behavior of EN AC-AlSi10Mg in boiling coolant with various average flow temperatures. *Materials and Corrosion, 66*(9) 931–939.

[21] Cabrini, M., Lorenzi, S., Pastore, T., Testa, C., Manfredi, D., Lorusso, M., Calignano, F., Pavese, M., & Andreatta, F. (2019). Corrosion behavior of AlSi10Mg alloy produced by laser powder bed fusion under chloride exposure. *Corrosion Science, 152*, 101–108. [CrossRef]

[22] Valentini, F., Pezzato, L., Dabala, M., & Brunelli, K. (2023). Study of the effect of functionalization with inhibitors on the corrosion properties of PEO-coated additive manufactured AlSi10Mg alloy. *Journal of Materials Research and Technology, 27*, 3595–3609. [CrossRef]

[23] Rafieazad, M., Chatterjee, A., & Nasiri, A. M. (2019). Effects of recycled powder on solidification defects, microstructure, and corrosion properties of DMLS fabricated AlSi10Mg. *Solidification Defects in Additive Manufactured Materials, 71*, 3241–3252. [CrossRef]

[24] Benbouzid, A. Z., Gharbi, O., Sidi-Yakoub, N., Tran, M. T. T., Turmine, M., & Vivier, V. (2023). Ionic liquid route for the corrosion inhibition of Al alloys: the effect of butylammonium nitrate on the corrosion of AA2024-T6. *Corrosion Communications, 9*, 57–64. [CrossRef]